Mol Genet Genomics (2017) 292:325–341
DOI 10.1007/s00438-016-1279-8

ORIGINAL ARTICLE

Genome-wide identification and functional analysis of S-RNase involved in the self-incompatibility of citrus

Mei Liang[1] · Wei Yang[1] · Shiying Su[1] · Lili Fu[1] · Hualin Yi[1] · Chuanwu Chen[2] · Xiuxin Deng[1] · Lijun Chai[1]

Received: 31 March 2016 / Accepted: 3 December 2016 / Published online: 8 December 2016

Abstract S-RNase-based self-incompatibility is found in Solanaceae, Rosaceae, and Scrophulariaceae, and is the most widespread mechanism that prevents self-fertilization in plants. Although 'Shatian' pummelo (*Citrus grandis*), a traditional cultivated variety, possesses the self-incompatible trait, the role of S-RNases in the self-incompatibility of 'Shatian' pummelo is poorly understood. To identify genes associated with self-incompatibility in citrus, we identified 16 genes encoding homologs of ribonucleases in the genomes of sweet orange (*Citrus sinensis*) and clementine mandarin (*Citrus clementine*). We preliminarily distinguished S-RNases from S-like RNases with a phylogenetic analysis that classified these homologs into three groups, which is consistent with the previous reports. Expression analysis provided evidence that *CsRNS1* and *CsRNS6* are S-like RNase genes. The expression level of *CsRNS1* was increased during fruit development. The expression of *CsRNS6* was increased during the formation of embryogenic callus. In contrast, we found that *CsRNS3* possessed several common characteristics of the pistil determinant of self-incompatibility: it has an alkaline isoelectric point (pI), harbors only one intron, and is specifically expressed in style. We obtained a cDNA encoding *CgRNS3* from 'Shatian' pummelo and found that it is homolog to *CsRNS3* and that *CgRNS3* exhibited the same expression pattern as *CsRNS3*. In an in vitro culture system, the CgRNS3 protein significantly inhibited the growth of self-pollen tubes from 'Shatian' pummelo, but after a heat treatment, this protein did not significantly inhibit the elongation of self- or non-self-pollen tubes. In conclusion, an S-RNase gene, *CgRNS3*, was obtained by searching the genomes of sweet orange and clementine for genes exhibiting sequence similarity to ribonucleases followed by expression analyses. Using this approach, we identified a protein that significantly inhibited the growth of self-pollen tubes, which is the defining property of an S-RNase.

Keywords Citrus · S-RNase · Phylogenetic analysis · Expression analysis · In vitro culture system · Self-incompatibility

Communicated by S. Hohmann.

Electronic supplementary material The online version of this article (doi:10.1007/s00438-016-1279-8) contains supplementary material, which is available to authorized users.

✉ Lijun Chai
chailijun@mail.hzau.edu.cn

[1] Key Laboratory of Horticultural Plant Biology, Ministry of Education, Key Laboratory of Horticultural Crop Biology and Genetic Improvement (Central Region), MOA, Huazhong Agricultural University, Wuhan 430070, Hubei, China

[2] Guangxi Academy of Specialty Crops, Guangxi Key Laboratory of Citrus Biology, Guangxi Academy of Specialty Crops, Guilin 541004, China

Introduction

Self-incompatibility is an important mechanism that inhibits fertilization by rejecting self-pollen and accepting non-self-pollen in bisexual flowering plants (De Nettancourt 2001). cDNA clones encoding the S-specific glycoprotein associated with self-incompatibility were first cloned from the gametophytic self-incompatible *Nicotiana alata* (Anderson et al. 1986). McClure et al. (1989) demonstrated that some of these glycoproteins share sequence similarity with the active sites of RNase T2 and RNase Rh. Thus, these glycoproteins are referred to as S-RNases (McClure

et al. 1989). Around the same time, S-RNases were successfully identified in species from Rosaceae, such as Japanese pear (Sassa et al. 1992, 1993), apple (Broothaerts et al. 1995), almond (Tao et al. 1997), and sweet cherry (Tao et al. 1999). Citrus, one of the most important evergreen perennials worldwide, contains both self-incompatible and self-compatible species (Ngo 2001; Masashi et al. 2006). However, the mechanism of self-incompatibility in citrus remains largely unknown relative to species from Rosaceae.

In citrus, the combination of self-incompatibility and parthenocarpy yields seedlessness, a highly favorable commercial trait. Thus, an increasing number of studies have focused on the mechanism of self-incompatibility in citrus. Genes that contribute to self-incompatibility in citrus were identified using comparative transcriptome approaches (Caruso et al. 2012; Miao et al. 2015; Zhang et al. 2015). Genes were previously associated with self-incompatibility in citrus, such as *CrWSKP1* and *CrS1-3*.15 from *Citrus reticulate* (Miao et al. 2011, 2013; Li et al. 2015), and *CgSL2*, *SKP1-like,* and *F-box* from *C. grandis* (Chai et al. 2010, 2011a, b). However, these genes are not essential for self-incompatibility, because they are not required for the rejection of S-allele-specific pollen. Many researchers suspect that the mechanism of self-incompatibility is similar in Citrus and Rosaceae in that the female determinant of self-incompatibility is an *S-RNase* gene (Miao et al. 2011; Chai et al. 2011b). However, no *S-RNase* genes that inhibit pollen tube growth have been discovered in citrus.

S-RNases belong to the RNase T2 family which catalyzes the cleavage of single-stranded RNA yielding oligonucleotides and mononucleotides. The RNase T2 family is divided into the S-RNases and S-like RNases subfamilies depending on whether the family members mediate the self-incompatibility response (Bariola and Green 1997). S-like RNases share structural features with S-RNases and are distributed throughout the kingdoms of life. Naturally, S-like RNases are associated with a broad range biological function, such as phosphate scavenging, antimicrobial defense, tRNA cleavage, and the enhancement of stress tolerance (Luhtala and Parker 2010). The expression of *RNS2* in Arabidopsis is induced under phosphate starvation. In addition, Pi remobilizing and cell senescence affect the expression of the apparent ortholog of *RNS2* from Antirrhinum, *AhSL28* (Taylor et al. 1993; Liang et al. 2002). The expression of several stress-induced S-like RNases associated with virus infection, drought, or mechanical wounding is induced to remarkably high levels in response to stress (Perez-Amador et al. 2002; Salekdeh et al. 2002; Ohno and Ehara 2005; Wei et al. 2006). Consistent with the evidently different roles of the S-RNases and S-like RNases in the evolution of plants, S-RNases and S-like RNases are classified into three groups based on the number of their introns and phylogenetic analyses (Igic and Kohn 2001). S-like RNases were assigned to groups I and II. S-RNases were assigned to group III.

In contrast to S-like RNases, S-RNases are specifically expressed in the style and inhibit the growth of pollen tubes as demonstrated by the genetic transformation of *Petunia inflata* and *Nicotiana* (Lee et al. 1994; Murfett et al. 1994). However, similar experiments are impractical for woody perennial species because of their long juvenile period. Therefore, testing whether candidate S-RNases possess S-RNase activity and surveying the downstream reactions induced by candidate S-RNases using an in vitro has become a common approach for identifying S-RNases from such species (Hiratsuka et al. 2001; Wang et al. 2009). The ribonuclease activity of S-RNase proteins is essential for self-incompatibility (Huang et al. 1994). After S-RNases are taken up by pollen tubes, they use the 26S proteasome pathway to specifically degrade the RNA of self-pollen tubes, which destroys the self-pollen tubes (McCubbin and Kao 2000; Takayama and Isogai 2005; Hua et al. 2008; Cui et al. 2014).

'Shatian' pummelo is an ancient species of the *Citrus* genus that exhibits self-incompatibility. We tested whether we could identify RNase T2 candidates in pummelo (*C. grandis*) using the genomic databases of sweet orange (*C. sinensis*) and clementine mandarin (*C. clementine*), because the genomic database of 'Shatian' pummelo is not available. To obtain candidate *S* genes associated with self-incompatibility, gene structure, sequence phylogeny, promoter elements, and expression patterns were analyzed to distinguish S-RNases from S-like RNases. Based on this analysis, we identified a candidate *S-RNase* and used the in vitro system to test the self-incompatible activity of this candidate S-RNase. Among the 16 RNase T2 homologs that we identified, one gene, *CgRNS3*, exhibited all of the characteristics of an S-RNase. *CgRNS3* was specifically expressed in pistil, and the protein encoded *CgRNS3* was found to specifically inhibit the growth of self-pollen tubes in an in vitro culture system.

Materials and methods

Plant materials

Fruit and embryogenic callus were used to test whether the RNase T2 genes might contribute to the development of fruit and embryos. We separately used two different genotypes of sweet orange (*C. sinensis*), because the late-ripening mutant and the embryonic callus from one genotype did not provide sufficient material for our experiments. The wild-type (WT) 'Fengjie 72-1' orange and its spontaneous late-ripening mutant (MT) 'Fengwan' were both

cultivated in the Fengjie orchard in Chongqing City, China. The sample fruits were harvested at 150, 170, 190, 210, and 240 days after flowering (DAF) from three different trees (Wu et al. 2014b) and then sliced. The non-embryogenic callus (NEC) of sweet orange was induced following the protocol of Deng's doctoral dissertation (Deng 1987). The embryonic callus was induced by culturing embryogenic callus (EC) on modified MT medium containing 2% (v/v) glycerol for 4 weeks (IEC4) (Liu and Deng 2002).

The tissues sampled from 'Shatian' pummelo (*C. grandis*) included young leaves and six different floral organs: petals, anthers, filaments, styles, ovaries, and pedicels, which were collected at the Citrus Research Institute (Guilin City, Guangxi, China) 10 days prior to anthesis (Liang et al. 2015). All of the samples were immediately frozen in liquid nitrogen and stored at −80 °C until further RNA and protein extractions. The anthers of 'Shatian' pummelo and Suan pummelo that were used for the in vitro pollen culture system were collected, dehisced, dried, and stored in a bottle containing desiccants at –40 °C.

In silico identification and sequence analysis of RNase T2 genes in citrus

The complete genomes and protein sequences of sweet orange (*C. sinensis*) and clementine mandarin (*C. clementine*) were separately downloaded from the *C. sinensis* genome database (http://www.citrus.hzau.edu.cn/orange/index.php) (Xu et al. 2013) and the phytozome database (http://www.phytozome.net/). The HMM profile of Ribonuclease T2 (PF00445_seed) was downloaded from the Pfam protein families database (http://www.pfam.xfam.org/), which was used as a query to identify the RNase T2 genes from sweet orange and clementine using HMMER 3.0 with an E-Value 1.0E−10. Each of the predicted genes was submitted to the SMART (http://www.smart.embl-heidelberg.de/) and Pfam (http://www.pfam.sanger.ac.uk/) databases to test whether they were bona fide members of the RNase T2 family.

The molecular weights (kDa) and isoelectric points (pI) of the proteins encoded by the predicted RNase T2 genes were calculated using the ProtParam tool at ExPASy (Gasteiger et al. 2005). The intron–exon structures were plotted using the Gene Structure Display Server (GSDS, http://www.gsds.cbi.pku.edu.cn/) based on the genomic sequences and the CDS sequences (Guo et al. 2007). Signal peptide regions were predicted using the SignalP 4.1 server (http://www.cbs.dtu.dk/services/SignalP/).

Multiple sequence alignment and phylogenetic analysis

Multiple sequence alignments for the amino-acid sequences of the 16 RNase T2 proteins were prepared using ClustalX (version 1.83). To distinguish the S-RNases from the S-like RNases, a phylogenetic analysis was performed with the 16 candidates and 74 RNase T2 enzymes (including 46 S-RNases and 28 S-like RNases) that were reported previously from diverse species and that were downloaded from the Uniprot database (http://www.uniprot.org/). The pertinent information for these 74 RNase T2 sequences is listed in Table S1. To avoid non-alignments caused by the excessive sequence divergence in the 5' and 3' ends, the regions between the first conserved position of the mature peptide and the last conserved cysteine residue were used for phylogenetic analyses (Igic and Kohn 2001). The phylogenetic tree was generated using MEGA5.0 (Tamura et al. 2011) using the neighbor-joining (NJ) method. The reliability test was carried out using 1000 bootstrap replications.

Promoter analysis of RNase T2 genes in citrus

To research the promoter sequences of the RNase T2 genes, 1,500 bp of genomic sequence that is upstream of the translational start site (ATG) was obtained from the sweet orange database. A draft containing all of the putative *cis*-acting motifs in these promoter-containing sequences was prepared by analyzing these sequences at the PlantCARE Website (http://www.intra.psb.ugent.be:8080/PlantCARE) (Lescot et al. 2002).

RNA extraction, semi-quantitative RT-PCR, and quantitative RT-PCR

Total RNA was extracted from fruit, embryogenic callus, leaves, and different floral organs as previously described by Liu and Liu. (Liu and Liu 2006). First-strand cDNA was synthesized from 2 μg of RNA using the RevertAid™ First-Strand cDNA Synthesis Kit (Fermentas, USA) according to the manufacturer's instructions. The specific primer pairs of semi-quantitative RT-PCR and quantitative RT-PCR were designed in non-conserved region with the software Primer 3, and were listed in Table S2. For quantitative RT-PCR, expression levels were normalized to the expression of *Actin* gene.

Semi-quantitative RT-PCR was conducted using a volume of 20 μL. Each semi-quantitative RT-PCR contained 600 ng of cDNA, 0.5 μM of each primer, 200 μM of each dNTP, and 2.5 U of Fast Pfu DNA Polymerase in 1× reaction buffer. PCRs were performed with an MJ-PTC-200 thermal controller (MJ Research, Waltham Mass) with the following steps: 94 °C for 10 min followed by 32 cycles of 94 °C for 16 s, 55 °C for 20 s, 72 °C for 20 s, and a final step at 72 °C for 10 min. The amplified products were analyzed using 2% agarose gels.

Quantitative RT-PCR analysis was performed in 10 μL reaction volumes with the ABI 7900HT Fast Real-Time

System with the SYBR Green PCR Master Mix. Each qRT-PCR contained 600 ng of cDNA and 0.5 μM of each primer in 1 × SYBR Green Mix. Quantitative RT-PCRs were performed with 384-well plates that included three biological replicates for each sample. The thermal cycling program began with an initial incubation at 50 °C for 2 min and an incubation at 95 °C for 1 min, followed by 40 cycles of 95 °C for 15 s followed by 60 °C for 1 min.

In vivo pollinations

To test the self-incompatibility of 'Shatian' pummelo, a 'Shatian' pummelo plant was self-pollinated at the Citrus Research Institute. In most self-incompatible varieties, pollen tubes reach the ovary at early bud stages, but as the style develops, their ability to grow is gradually reduced (Chalivendra et al. 2013). After the anthers were removed, styles at different developmental stages (stage 1: 5 days before flowering, stage 2: 4 days before flowering, stage 3: 3 days before flowering, stage 4: 2 days before flowering, stage 5: 1 day before flowering) were pollinated with mature self-pollen that was collected in 2014. Pistils were collected after 3 days and were immediately fixed in formalin/acetic acid/alcohol (FAA). After fixing, the pistils were stained with the aniline blue fluorochrome as described by Lin et al. (Lin et al. 2015).

Antibody generation, protein extraction, and western blot analysis

A cDNA clone derived from *CsRNS3* mRNA was obtained by PCR-mediated amplification of cDNA prepared from the styles of 'Shatian' pummelo. This cDNA sequence of *CgRNS3* is available from genbank (accession number KX894564). The coding sequence of *CgRNS3*, without the signal peptide, was inserted into the pEASY blunt E1 expression vector (TransGen). The recombinant protein was expressed in *Escherichia coli* strain BL21 (DE3) (TransGen), purified, and used to develop anti-CgRNS3 antisera in rabbits. Total protein was extracted from the young leaves and six floral organs (petals, anthers, filaments, styles, ovaries, and pedicels) from 'Shatian' pummelo as described previously (Isaacson et al. 2006; Pan et al. 2009). The concentration of protein in these extracts was determined with a modified Bradford protein assay kit (Sangon Biotech) using bovine serum albumin (BSA) as standard. Equal amounts of protein (20 μg) were analyzed using SDS-PAGE. The 10% gels were analyzed by immunoblotting using polyvinylidene difluoride (PVDF) membranes, as previously described (Cao et al. 2012). The anti-CsRNS3 antisera were diluted 1:1000; the anti-actin antibodies (ABclonal) were diluted 1:5000. The appropriate secondary antibodies were diluted 1:2500. The immunoreactive bands were detected using the ECL plus western blot detection kit (GE Healthcare).

Recombinant protein expression and RNase activity assay

To obtain massive quantities of the recombinant CgRNS3 protein, the mature protein (i.e., lacking the signal peptide) was expressed as a GST-fusion protein using the pGEX-6P-1 expression vector, because GST tags enhance the expression level (Waugh 2005). The GST-CgRNS3 fusion protein was expressed in *Escherichia coli* strain BL21 (DE3) (TransGen). The strain was grown at 37 °C in LB medium containing ampicillin at a concentration of 100 μg/mL. When the OD_{600} of the suspension reached 0.6, the bacteria were transferred to fresh LB medium containing ampicillin at a concentration of 100 μg/mL with a 1:100 dilution. The expression of the GST-CgRNS3 fusion protein was induced with 0.25 mM IPTG at 16 °C for 20 h. The cells were lysed using sonication in binding buffer (containing 140 mM NaCl, 2.7 mM KCl, 10 mM Na_2HPO_4, 1.8 mM KH_2PO_4, 2 mM DTT, pH 7.3). The fusion protein was purified using glutathione Sepharose 4B beads (GE Healthcare) according to the manufacturer's protocol. Protein concentrations were estimated using the Bradford assay using BSA as a standard. The RNase activity of the recombinant protein was assayed using torula yeast RNA (Sigma) as substrate as previously described (Nishimura et al. 2014). Sodium citrate buffers with pH values ranging from 3 to 9 were used to test the pH optimum. To test the subcellular localization of CgRNS3, a cDNA encoding the full-length CgRNS3 protein was inserted into pM999-GFP and transiently expressed in protoplasts that were isolated from citrus leaves according to the protocol of Yoo et al. (Yoo et al. 2007). GFP fluorescence was imaged using a confocal laser scanning microscope.

In vitro pollen culture and S-RNase inhibition assay

Pollen grains were cultured in liquid germination medium (GM) which contained 0.02% $MgSO_4$, 0.01% KNO_3, 0.03% $Ca(NO_3)_2$, 0.01% H_3BO_3, 15% PEG-4000, and 20% sucrose at pH 6.0. After the recombinant GST-CgRNS3 was added to the basal GM at concentrations of 25, 50, and 100 μg/mL, pollen was uniformly scattered onto the GM and incubated in a dark and humid chamber for 9 h at 28 °C. Three independent experiments were performed for each treatment. Images of the pollen were acquired using light microscopy. At least 150 pollen tubes were measured for each treatment using the image pro-plus software.

Table 1 Characteristics of putative RNase T2 genes from sweet orange (*Citrus sinensis*)

Name	ID	Chr	CDs	Amino acid	MW (kDa)	pI
CsRNS1	Cs2g18380.1	2	843	280	31.7	5.28
CsRNS2	Cs2g26150.1	2	675	224	25.9	9.39
CsRNS3	Cs2g26130.1	2	669	222	25.7	9.37
CsRNS4	Cs3g07430.1	3	678	225	25.6	8.85
CsRNS5	Cs7g03770.1	7	693	230	25.8	5.3
CsRNS6	Cs7g03760.1	7	681	226	25.8	5.14
CsRNS7	Orange1.1t03886.1	un	708	235	26.7	9.21
CsRNS8	Orange1.1t03889.1	un	384	127	14.3	7.67
CsRNS9	Orange1.1t03891.1	un	666	221	25.3	9.82

Table 2 Characteristics of putative RNase T2 genes from clementine mandarin (*Citrus clementine*)

Name	ID	Chr	CDs	Amino acid	MW (kDa)	pI
ClRNS1	Ciclev10016242 m	Scaffold_2	819	272	30.2	5.36
ClRNS2	Ciclev10032651 m	Scaffold_4	693	230	25.8	5.47
ClRNS3	Ciclev10032660 m	Scaffold_4	687	228	25.7	5.47
ClRNS4	Ciclev10032674 m	Scaffold_4	681	226	25.8	5.14
ClRNS5	Ciclev10003503 m	Scaffold_5	666	221	25.4	9.91
ClRNS6	Ciclev10003955 m	Scaffold_5	711	236	26.9	8.65
ClRNS7	Ciclev10027322 m	Scaffold_7	423	140	16.3	9.72

Results

In silico identification and characterization of RNase T2 genes

To identify the RNase T2 genes in the genomes of citrus, we used the Hidden Markov Model (HMM) profile of the Pfam RNase T2 domain as a query in a BLASTP search of the available sweet orange and clementine mandarin genomes. We identified 9 and 7 RNase T2 homologs from sweet orange and clementine mandarin, respectively, which we named *CsRNS1* through *CsRNS9* and *ClRNS1* through *ClRNS7* (Tables 1, 2). The calculated molecular weights for the proteins encoded by these 16 putative RNase T2 genes mostly ranged from 25 to 32 kDa, which is typical for RNase T2 enzymes (Deshpande and Shankar 2002). The calculated molecular weights of the proteins encoded by *CsRNS8* and *ClRNS7* were outside of this range (14.3 and 16.3 kDa, respectively). We calculated acidic pI values for 7 and basic pI values for eight of these putative RNase T2 enzymes. We calculated a nearly neutral pI value for only the RNase T2 enzyme encoded by *CsRNS8* (Tables 1, 2).

Multiple sequence alignments of the full-length amino-acid sequences of these putative RNase T2 proteins indicated that all of these proteins, with the exception of CsRNS8, ClRNS1, and ClRNS7, contained two conserved active site (CAS I and CAS II) histidine residues that are essential for RNase T2 activity (Kawata et al. 1990) (Fig. S1). The coding sequences of CsRNS8 and ClRNS7 were short (approximately 400 bp) relative to the *CsRNS* and *ClRNS* sequences that contained both CAS I and CAS II. In CsRNS8 and ClRNS7, the CAS I motif was lost. The sequence identity between CsRNS1 and ClRNS1 is 84%. However, the deletion of a short sequence close to the CAS II motif was observed in ClRNS1 (Fig. S1). All the proteins also had half-cystine residues with different levels of conservation, which form disulfide bridges to promote the proper folding of protein tertiary structure (Irie 1999).

Phylogenetic analysis of RNase T2 genes in citrus

A phylogenetic tree was constructed with the 16 *CsRNS* and *ClRNS* genes using the MEGA program and the neighbor-joining (NJ) method. This analysis separated these genes into three groups (Fig. 1a). To further understand the relationships among these RNase T2 genes, the GSDS program was used to determine their intron–exon structures. We found that the genes that clustered into the same subgroups shared similar intron–exon structures. Genes that clustered into group I have only one intron, with the exceptions of *CsRNS8* and *ClRNS7*, which have no intron. *CsRNS1* and *ClRNS1* have seven and six introns, respectively, and formed an independent cluster. The members of group III, namely *CsRNS5*, *CsRNS6*, *ClRNS2*, *ClRNS3,* and *ClRNS4*, each have three introns. Our phylogenetic tree and our findings on the intron–exon structures of these genes

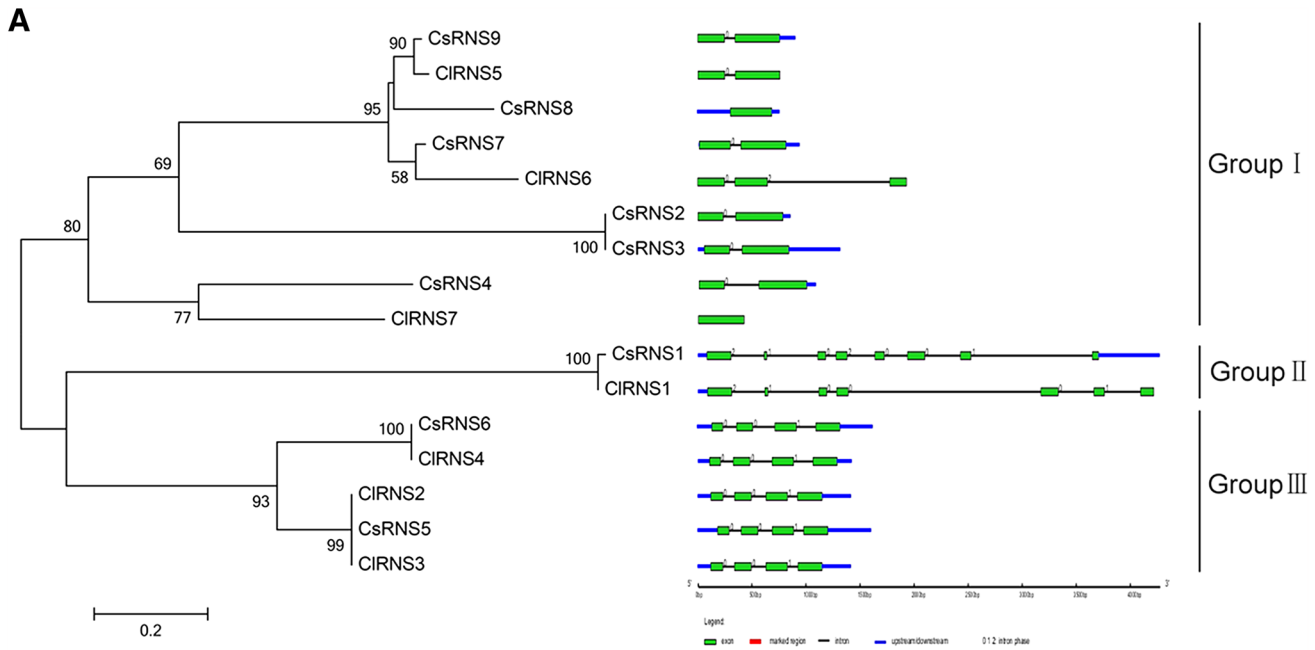
A
CsRNS9
ClRNS5
CsRNS8
CsRNS7
ClRNS6
CsRNS2
CsRNS3
CsRNS4
ClRNS7
CsRNS1
ClRNS1
CsRNS6
ClRNS4
ClRNS2
CsRNS5
ClRNS3
90
95
58
69
80
100
100
77
100
100
93
99
0.2
Group Ⅰ
Group Ⅱ
Group Ⅲ

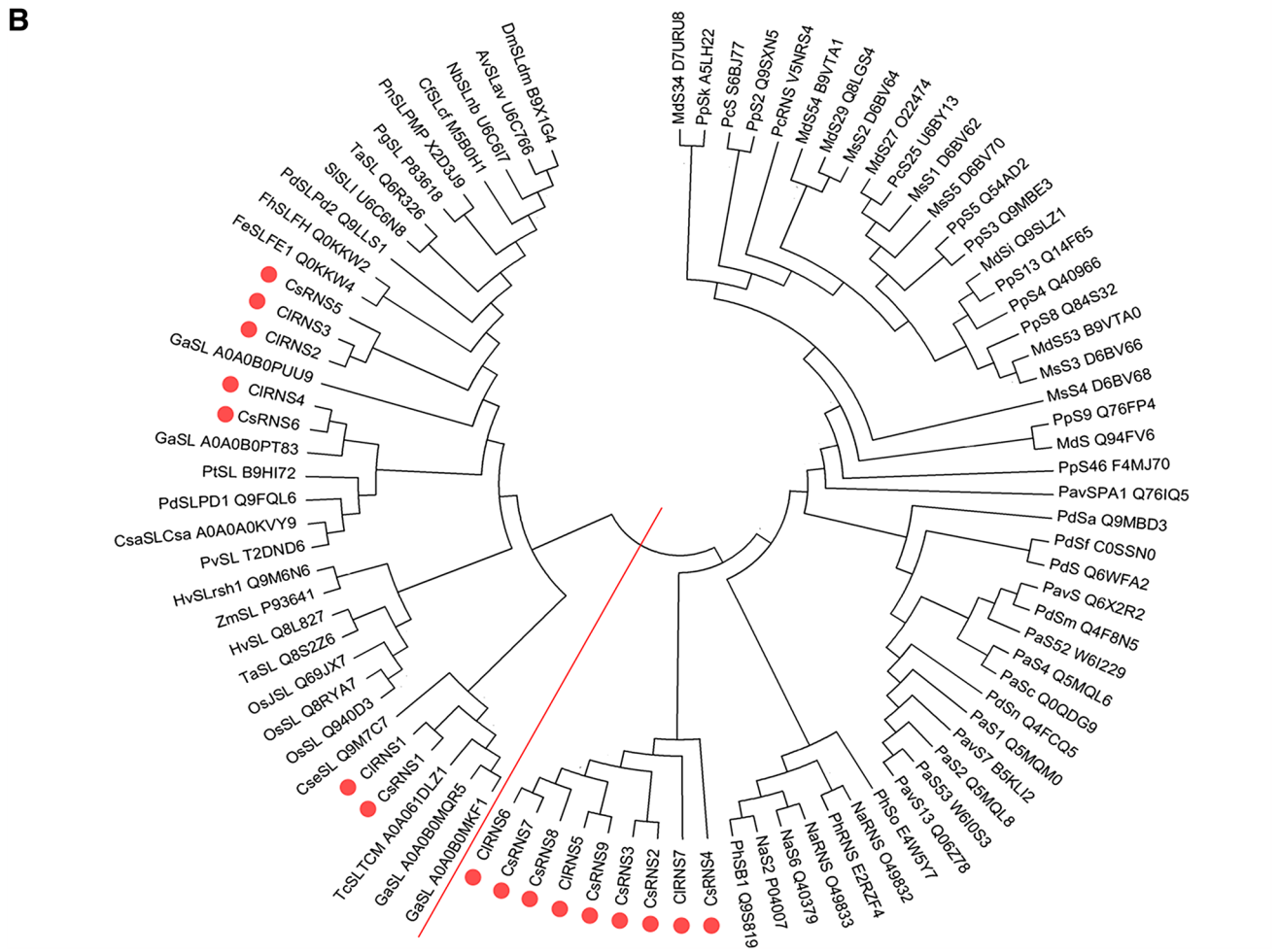
B
DmSLdm B9X1G4
AvSLav U6C766
NbSLnb U6C6I7
CfSLcf M5B0H1
PnSLPMP X2D3J9
PgSL P83618
TaSL Q6R326
SlSLI U6C6N8
PdSLPd2 Q9LLS1
FhSLFH Q0KKW2
FeSLFE1 Q0KKW4
CsRNS5
ClRNS3
ClRNS2
GaSL A0A0B0PUU9
ClRNS4
CsRNS6
GaSL A0A0B0PT83
PtSL B9HI72
PdSLPD1 Q9FQL6
CsaSLCsa A0A0A0KVY9
PvSL T2DND6
HvSLrsh1 Q9M6N6
ZmSL P93641
HvSL Q8L827
TaSL Q8S2Z6
OsJSL Q69JX7
OsSL Q8RYA7
OsSL Q940D3
OsSL Q9M7C7
CseSL Q9M7C7
ClRNS1
CsRNS1
TcSLTCM A0A061DLZ1
GaSL A0A0B0MQR5
GaSL A0A0B0MKF1
ClRNS6
CsRNS7
CsRNS8
ClRNS5
CsRNS9
CsRNS3
CsRNS2
ClRNS7
CsRNS4
PhSB1 Q9S819
NaS2 P04007
NaS6 Q40379
NaRNS Q49833
PhRNS E2RZF4
PhSo E4W5Y7
PavS13 Q06Z78
PaS53 W6I0S3
PaS2 Q5MQL8
PavS7 B5KLI2
PaS1 Q5MQM0
PdSn Q4FCQ5
PaSc Q0QDG9
PaS4 Q5MQL6
PaS52 W6I229
PdSm Q4F8N5
PavS Q6X2R2
PdS Q6WFA2
PdSf C0SSN0
PdSa Q9MBD3
PavSPA1 Q76IQ5
PpS46 F4MJ70
MdS Q94FV6
PpS9 Q76FP4
MsS4 D6BV68
MsS3 D6BV66
MdS53 B9VTA0
PpS8 Q84S32
PpS4 Q40966
PpS13 Q14F65
MdSi Q9SLZ1
PpS3 Q9MBE3
PpS5 Q54AD2
MsS5 D6BV70
MsS1 D6BY13
PcS25 U6BY13
MdS27 Q22474
MsS2 D6BV64
MdS29 Q8LGS4
MdS54 B9VTA1
PcRNS V5NRS4
PpS2 Q9SXN5
PcS S6BJ77
PpSk A5LH22
MdS34 D7URU8

◂**Fig. 1** Phylogenetic analysis of 16 RNase T2 genes from citrus. **a** The phylogenetic tree and gene structures were generated using MEGA5.0 and GSDS, respectively. All of the RNase T2 genes tested were clustered into three distinct groups. Exons and introns are depicted by filled *green boxes* and *single lines*, respectively. **b** Phylogenetic relationships among 16 RNase T2 and 74 RNase T2 enzymes from diverse species. The tree was constructed using the neighbor-joining algorithm using the MEGA5.0 program. The reliability of this tree was inferred from a bootstrap analysis of 1000 replicates. The RNase T2 genes identified in this study are indicated with filled *red circles*

are consistent with the findings of the previous publication (Igic and Kohn 2001).

Next, we analyzed the phylogenetic relationships among the 16 putative RNase T2 genes and the other homologs to determine whether these putative RNase T2 genes encode S-RNases or S-like RNases. Thus, 46 S-RNase and 28 S-like RNase protein sequences were randomly collected from the UniProt database and a phylogenetic tree was constructed with the amino-acid sequences of the predicted mature proteins and the amino-acid sequences encoded by the 16 putative RNase T2 genes described above (Fig. 1b). We found that the S-RNases from Rosaceae and Solanaceae and some of the predicted RNase T2 enzymes clustered together and that the RNase T2 genes from citrus were more closely related to the S-RNases from Solanaceae than to the S-RNases from Rosaceae. Another branch contained *CsRNS1*, *CsRNS5*, *CsRNS6*, and *ClRNS1,* through *ClRNS4*, and the 28 S-like RNase sequences that we analyzed from various species (Fig. 1b). This phylogenetic analysis provides evidence that some of these putative RNase T2 genes might serve as S-RNases that contribute to the self-incompatibility reaction. In addition, we found that each putative RNase T2 gene from clementine mandarin and one RNase T2 gene from sweet orange comprised one subgroup (Fig. 1a, b). These data provide evidence that these putative RNase T2 genes from clementine and sweet orange perform the same reaction in vivo. On the other hand, pummelo share greater sequence identity with sweet orange than that with clementine, because sweet orange is a hybrid between pummelo and mandarin (Xu et al. 2013; Velasco and Licciardello 2014; Wu et al. 2014a). Hence, we decided to test the possible biological functions of *CsRNS1* through *CsRNS9*.

Stress-relevant *cis*-elements in the promoters of RNase T2 genes

S-like RNases often contribute to stress tolerance in plants. To identify the possible stress-related *cis*-elements in the promoter regions, we analyzed the 1500 bp located upstream of the translational start sites of *CsRNS1 through CsRNS9* using the PlantCARE database. All the identified elements are displayed in Fig. S2. CAAT-boxes and TATA-boxes were highly conserved among the nine genes. As shown in Table 3, 15 types of stress-related *cis*-acting motifs were detected, and these motifs included the anaerobic induction element (ARE), fungal elicitor element (Box-W1), heat stress responsive element (HSE), drought inducibility element (MBS), low-temperature responsive element (LTR), defense and stress responsive element (TC-rich repeats), and multiple *cis*-acting elements that respond to hormones. Among all the different *cis*-elements that we identified, the MBS and TC-rich repeats were the most abundant, accounting for 32% of all the identified elements. The promoter of each putative RNase-encoding gene that we tested had at least one MBS element. The majority of the promoters among the putative RNase T2 genes possessed ten or more elements. We identified 19 cis-elements in *CsRNS1*, which was the maximum number of elements that we identified in any of the genes that we tested. Almost half of the elements (8/19 *cis*-elements) that we identified in the promoter of *CsRNS1* were reported to respond to MeJA (Table 3).

Expression analysis of RNases under diverse biological processes

To obtain evidence for the biological functions of these RNase T2 genes, we tested their expression levels during embryogenesis and in different developmental stages of fruit. Morphological changes could be clearly observed among non-embryogenic callus (NEC), callus induced for 4 weeks (IEC4) and embryogenic callus (EC) (Fig. 2). Results from semi-quantitative PCR experiments revealed that only *CsRNS3* and *CsRNS6* were expressed during embryo development *CsRNS3* was detected in the NEC and EC stages. There was no significant difference in the levels of expression of *CsRNS3* during these two stages of development. *CsRNS6* showed a prominent band at the EC stage but undetectable or weak expression at the NEC stage. In addition, quantitative RT-PCR was performed on RNA extracted from fruits harvested 150, 170, 190, 210, and 240 DAF in a spontaneous late-ripening orange mutant (MT) and its wild type (WT) (Fig. 3). In MT, the expression levels of 4 RNases (*CsRNS1*, *CsRNS2*, *CsRNS3*, *CsRNS7,* and *CsRNS8*) in MT significantly increased at 240 DAF and were obviously higher than in WT. It is noteworthy that the expression levels of *CsRNS1* were continuously up-regulated during fruit ripening in MT and the WT and that in contrast, no difference were observed in the expression levels of *CsRNS4*, *CsRNS5*, *CsRNS6,* and *CsRNS9* during fruit ripening in MT and the WT.

Table 3 Types and numbers of stress-related elements in the promoter regions of RNase T2 genes

Element	ARE	Box-W1	HSE	MBS	LTR	TC-rich repeats	CGTCA motif	TGACG motif	ERE	TCA element	ABRE	GARE motif	P-box	TATC-box	TGA element	Total
Function	Anaerobic induction	Fungal elicitor	Heat stress	Drought	Low temperature	Defense and stress	MeJA		Ethylene	Salicylic acid	Abscisic acid	Gibberellin			Auxin	
CsRNS1	2	2	1	4		2	4	4								19
CsRNS2	1		3	2		2			1	1						10
CsRNS3	1		3	2		2			1	1						10
CsRNS4	1			1		1	1	1			1	1				7
CsRNS5	1		1	2		3	1	1		1	1				1	12
CsRNS6				3	1		1	1		1	1		1		1	10
CsRNS7	1	2	2	1		2				1	1			1		11
CsRNS8	1	2	1	2		1	1	1		1	2	1		1		14
CsRNS9	1	1	1	1		1				1				1		7
Total	9	7	12	18	1	14	8	8	2	7	6	2	1	3	2	100

Tissue specific analysis of RNases

The defining characteristics of S-RNases are (1) they are specifically expressed in the style and (2) they participate in the self-incompatible reaction in Solanaceae, Rosaceae, and Scrophulariaceae (McClure et al. 1989). As shown in Fig. 4a, the length of self-pollen tubes was gradually shortened during the development of stigma and ultimately the tube stopped growing at the 1/3 position of the style. These data are consistent with 'Shatian' pummelo possessing a self-incompatibility system. To test whether some of the predicted RNases in our study might contribute to self-incompatibility, the levels of their expression were estimated in the leaves and in six floral organs of 'Shatian' pummelo using semi-quantitative PCR (Fig. 4b). *CsRNS1* was highly expressed in all the sampled organs. In contrast, the expression levels of *CsRNS4* and *CsRNS9* were below the limits of detection in all of the tissues tested. *CsRNS5*, *CsRNS6*, *CsRNS7*, and *CsRNS8* were expressed in multiple tissues. In contrast, *CsRNS3* was specifically expressed in style, and *CsRNS2* was specifically expressed in the pistil.

Cloning and function of *CgRNS3*

Based on the results of our phylogenetic and expression analyses, we concluded that *CsRNS3* is potentially an S-RNase that contributes to self-incompatibility in citrus. A cDNA encoding *CgRNS3* (*C. grandis* RNase 3) synthesized from mRNA extracted from the styles of 'Shatian' pummelo was cloned and sequenced. There was 99% sequence identity between *CgRNS3* and *CsRNS3*. The signal peptide of CgRNS3 was followed by a special structural domain found in type T2 RNases and a single intron was inserted into the hypervariable region (Fig. 5). The CgRNS3 protein shares the conserved regions C1, C2, C3, and C5, but the C4 region was different from the S-RNases from Solanaceae and Rosaceae. CgRNS3 is similar to Rosaceae S-RNases, which have only one hypervariable region named RHV, and is distinct from Solanaceae S-RNases in that Solanaceae S-RNases have two hypervariable regions (HVa and HVb) (Fig. 5).

We used quantitative RT-PCR and western blot analyses to test the expression levels of *CgRNS3* in the different tissues of 'Shatian' pummelo, and found that *CgRNS3* was expressed at high levels in the style (Fig. 6). To test whether CgRNS3 participates in the self-incompatible reaction, we first prepared recombinant CgRNS3 protein by fusing the full-length cDNA without the signal peptide to GST in pGEX-6P-1 and expressed the fusion protein in *E. coli* (Fig. 7a). The ribonuclease activity and pH optimum of the recombinant CgRNS3 were tested using torula yeast RNA as the substrate. RNase activity was quantified at several different pH values ranging from 3 to 9. The activity

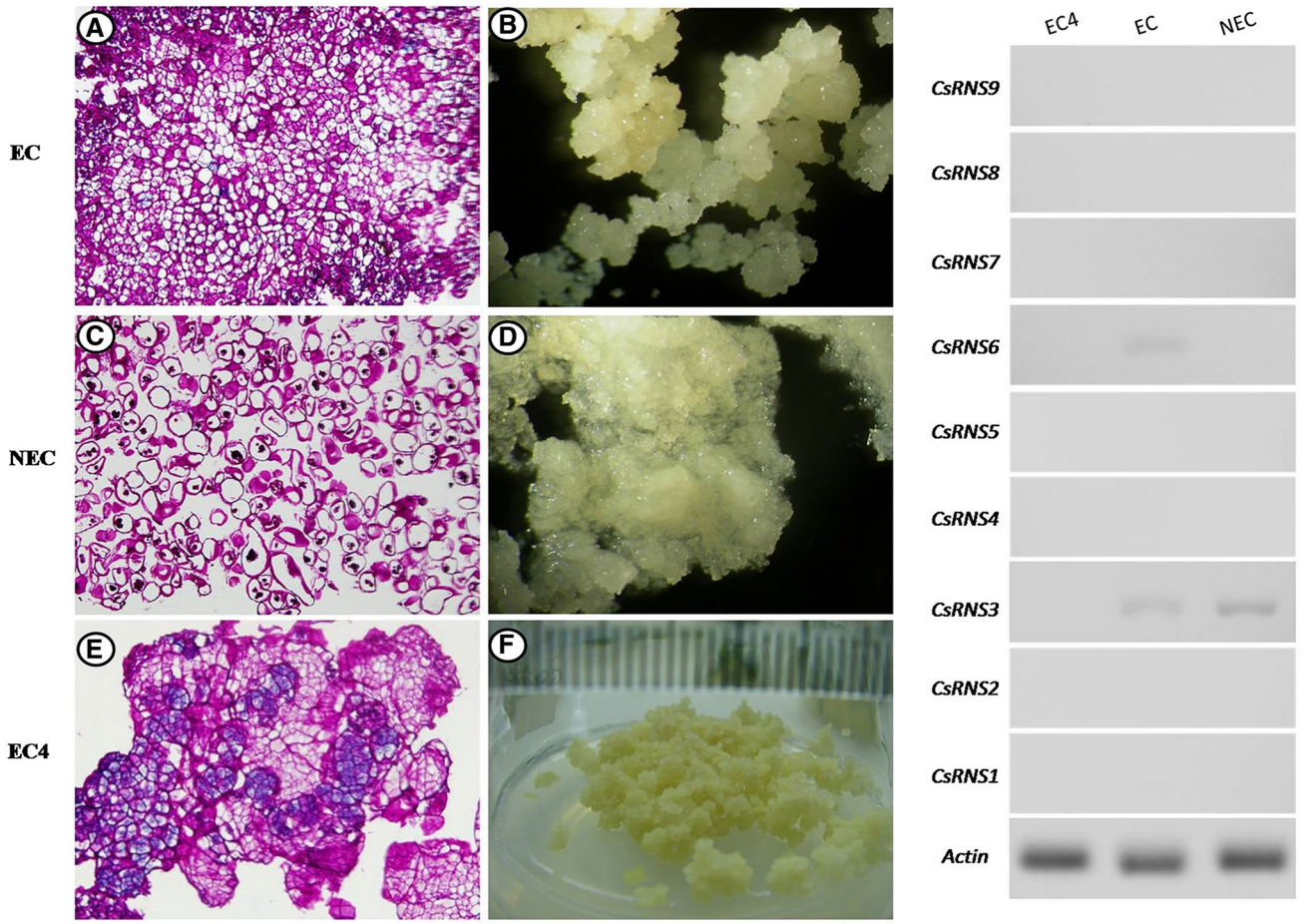

Fig. 2 Expression patterns of *CsRNS1* through *CsRNS9* in three different callus tissues from sweet orange. Total RNA was extracted from embryogenic callus (EC), non-embryogenic callus (NEC), and embryogenic callus induced for 4 weeks (EC4). Gene expression was evaluated by semi-quantitative RT-PCR. Amplification of actin was used as a loading control

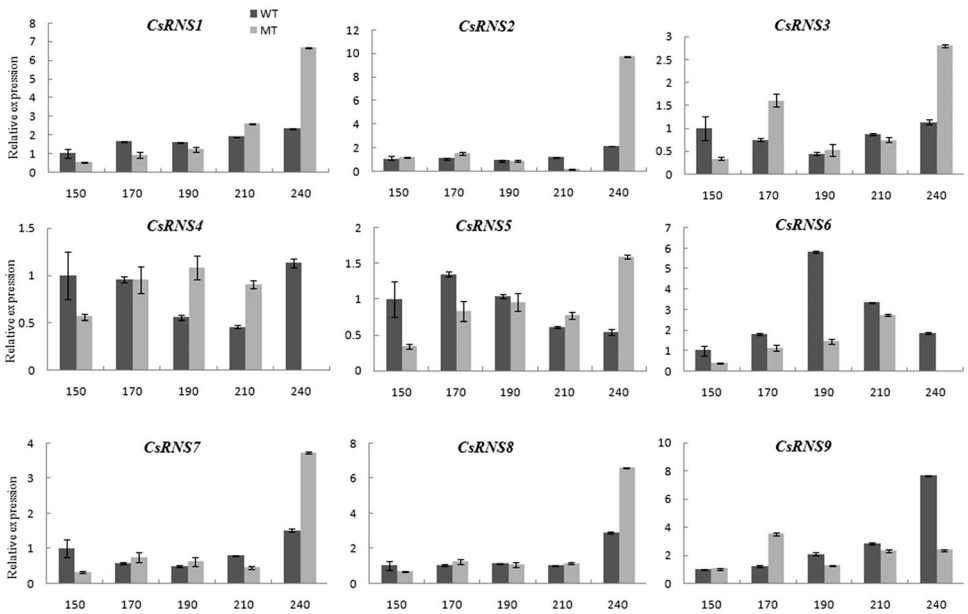

Fig. 3 Expression patterns of *CsRNS1* through *CsRNS9* in the fruit of a spontaneous late-ripening orange mutant (MT) and the relevant wild type (WT). The developmental stages of fruit ripening that were tested included 150, 170, 190, 210, and 240 day after flowering. Quantitative RT-PCR was used to quantify mRNA levels. Three biological replicates were analyzed for the MT and the WT. *Error bars* indicate standard deviation

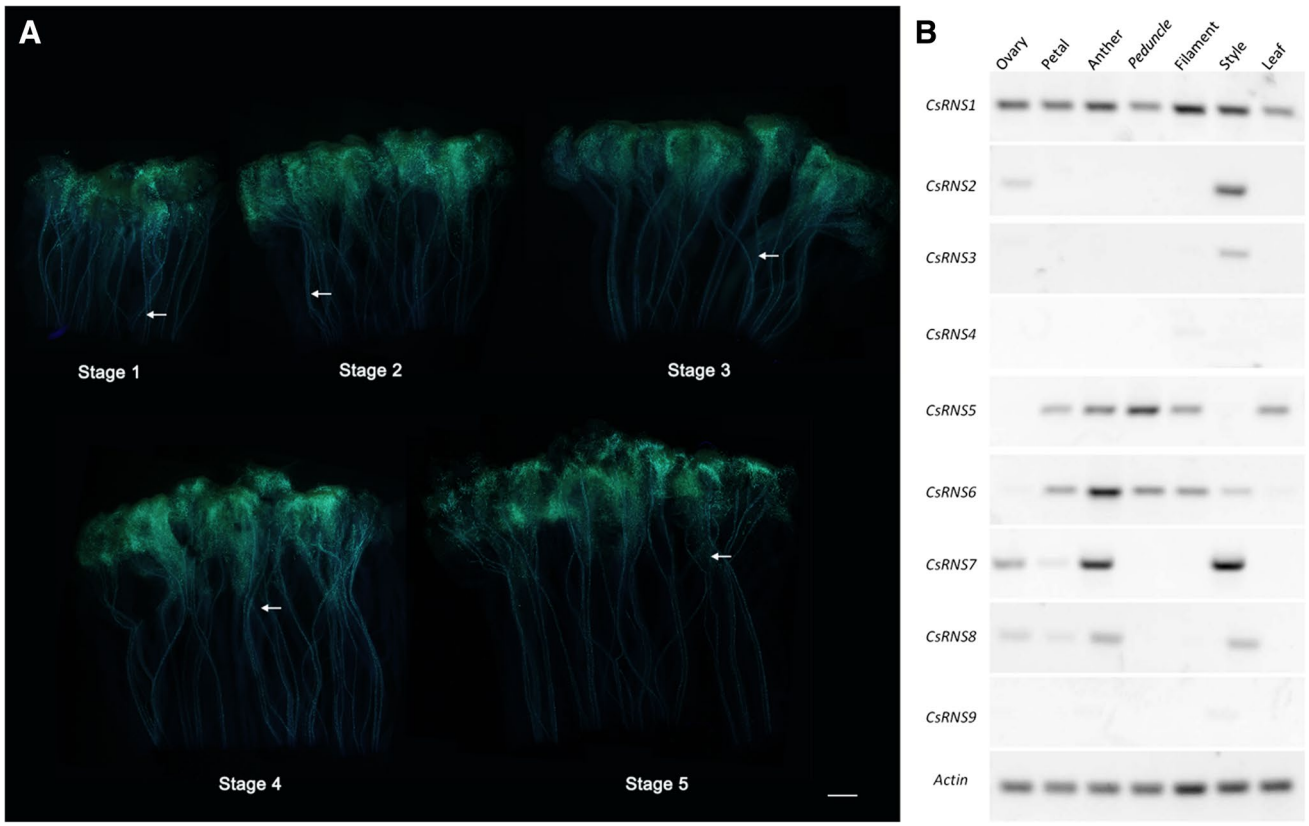

Fig. 4 Expression patterns of *CsRNS1* through *CsRNS9* in 'Shatian' pummelo (*Citrus grandis*). **a** Aniline blue staining of self-pollinated 'Shatian' pummelo pistils at different developmental stages. The position of pollen tube inhibition is indicated with an *arrow*. *Bar* 1 cm. **b** Semi-quantitative RT-PCR in seven different tissues from 'Shatian' pummelo. Leaves and six flower tissues dissected from mature flowers (ovary, petal, anther, peduncle, filament, and style) were analyzed. Amplification of actin was used as a loading control

of RNase A was also tested in these assays, for a comparison. RNase A exhibited the highest activity at an acidic pH value. We found that the recombinant CgRNS3 protein possessed ribonuclease activity. In contrast to RNase A, the recombinant CgRNS3 exhibited optimum activity at pH 8 (Fig. 7b). Moreover, the subcellular localization of *CgRNS3* indicated that it was a cytoplasm protein (Fig. 7c).

To confirm whether *CgRNS3* was functionally involved in the self-incompatibility response, we added CgRNS3 to the in vitro culture system at three different concentrations: 25, 50, and 100 μg/mL. In production, the pollen from Suan pummelo is always used to pollinate 'Shatian' pummelo because of the self-incompatibility problem in 'Shatian' pummelo. Thus, we reasoned that in theory, the pollen from Suan pummelo should develop normally in an in vitro culture system programmed with pistils from 'Shatian' pummelo. Indeed, we found that the phenotype of the non-self-pollen tube appeared relatively normal in the in vitro culture system (Fig. 8a). In addition, we observed that most of the self-pollen tubes exhibited a curved apex when CgRNS3 was present at 25 μg/mL. This abnormal phenotype was enhanced when the concentration of CgRNS3 was increased. However, the phenotype of curved apex was almost no detection in non-self-pollen tube (Fig. 8a). Based on measurements of pollen tube length, the inhibitory effect on the growth of the pollen tubes was not obvious for both self- and non-self-pollen tubes when the CgRNS3 protein concentration was 25 μg/mL. However, the CgRSN3 protein strongly inhibited the growth of both types of pollen tubes when the protein concentration exceeded 25 μg/mL. Interestingly, when the CgRNS3 protein was present at 100 μg/mL, we observed a 59% reduction in the length of the tubes of 'Shatian' pummelo. In contrast, when the CgRNS3 protein was present at 100 μg/mL, we observed a 47% reduction in the tubes of Suan pummelo. After the protein was heated, it no longer induced the curved apex phenotype in the self-pollen tubes and the inhibition of pollen tube growth was alleviated (Fig. 8a, b). In summary, *CgRNS3* appears to be an S-RNase, because *CgRNS3* has the characteristic structural and expression pattern of an S-RNase and similar to other reported S-RNases *CgRNS3* possessed ribonuclease

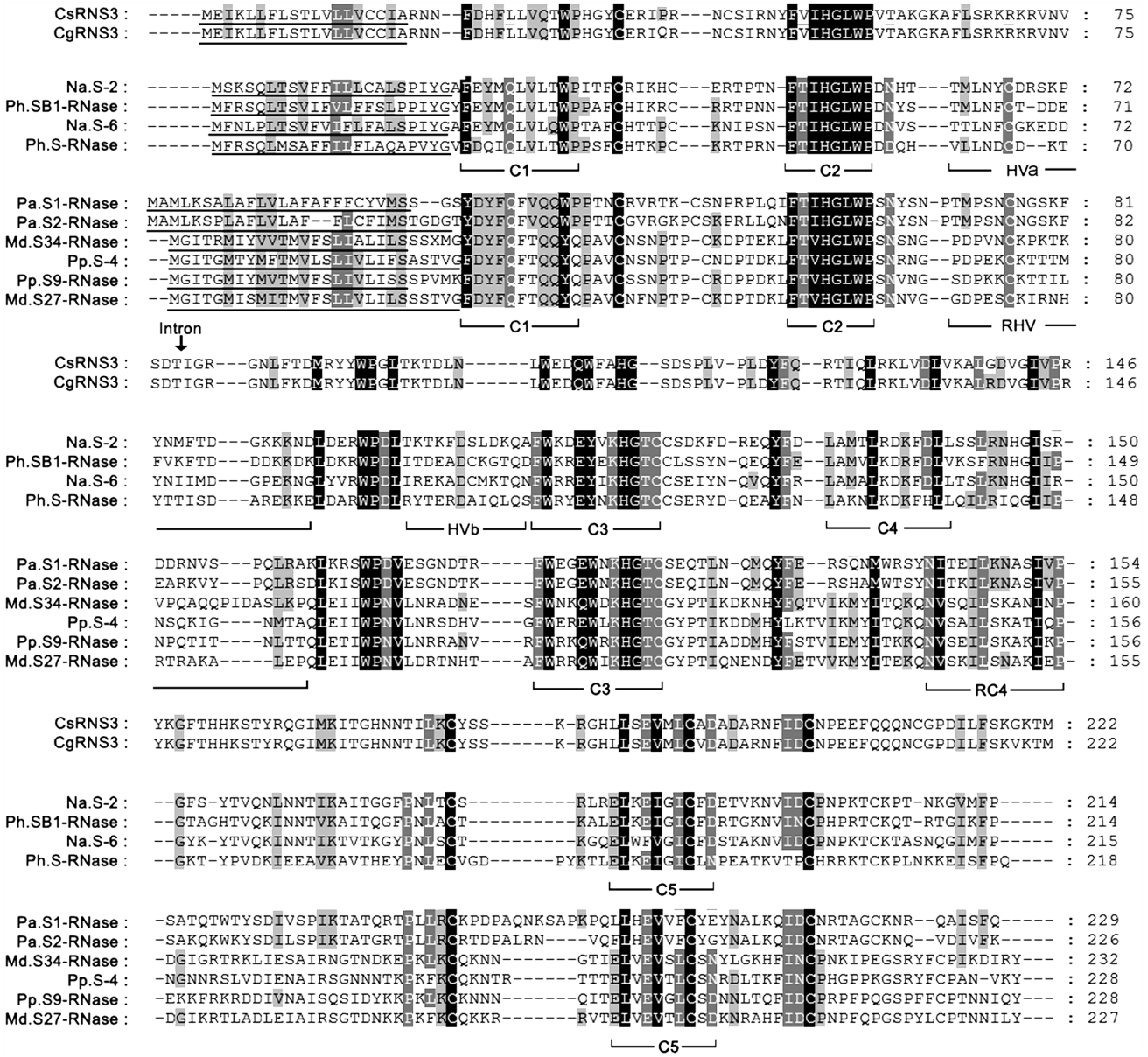

Fig. 5 Amino-acid sequence alignment of the S-RNases from citrus and other species. The conserved regions and the hypervariable regions of the S-RNases from Solanaceae and Rosaceae are indicated under the corresponding sequences. The position of the intron is inserted in the gene encoding CgRNS3 which is marked with an arrow and the signal peptide is indicated with a straight line. The reported S-RNase sequences are from *Nicotiana alata*, *Petunia hybrid*, *Malus domestica*, *Pyrus pyrifolia,* and *Prunus armeniaca*

activity and inhibited the growth of self-pollen in the in vitro culture system.

Discussion

Identification and classification of RNase T2 in citrus

RNase T2 genes perform a variety of functions in diverse prokaryotic and eukaryotic organisms. Recently, the publication of abundant genetic and genomic information for sweet orange and clementine mandarin have facilitated a better understanding of many biological traits in citrus (Xu et al. 2013; Wu et al. 2014a). Here, we report on the identification of 9 and 7 RNase T2 homologs from the sweet orange and clementine mandarin databases, respectively (Tables 1, 2). Based on our phylogenetic analysis, we conclude that each of the putative RNase T2 genes from clementine mandarin is closely related to one of the putative RNase T2 genes from sweet orange (Fig. 1a, b). Plant

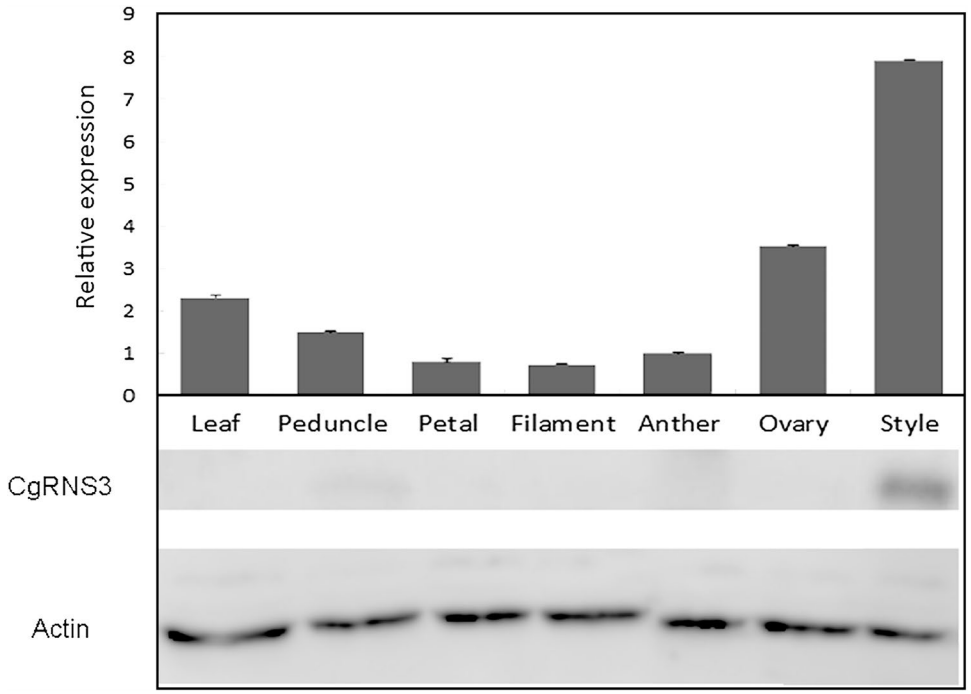

Fig. 6 Expression of CgRNS3 in the different tissues of 'Shatian' pummelo. Expression levels were analyzed using quantitative RT-PCR and western blotting. Plant actin was used as internal reference. Three biological replicates were analyzed. *Error bars* indicate standard deviation

RNases T2 genes were classified into three major groups based on the previous phylogenetic analyses and the number of introns in these genes (Igic and Kohn 2001). The S-like RNases are in groups I and II. The genes in group I have two or three introns. The genes in group II have seven or more introns. The S-RNases are in group III and have only one intron (Lee et al. 1992; Igic and Kohn 2001; Roalson and McCubbin 2003; Banović et al. 2009). Our phylogenetic analysis indicated that all of the candidate RNases T2 genes that we identified in this study were also classified into three groups. The numbers of introns in the genes from these groups are consistent with the previous findings (Fig. 1a). The genes with three introns (*CsRNS5* and *CsRNS6*) and the single gene with seven introns (*CsRNS1*) formed a single cluster. The *CsRNS2/3/4/7/8/9* genes have only one intron or no introns (*CsRNS8*) formed a distinct cluster. Moreover, we obtained the same results with the phylogenetic tree constructed with 74 RNase T2 homologs and also found that *CsRNS1*, *CsRNS5,* and *CsRNS6* clustered with the 28 S-like RNases. The other predicted RNase T2 genes in sweet orange clustered with the S-RNases from Rosaceae and Solanaceae (Fig. 1b). Thus, our analysis appeared to distinguish S-RNases and S-like RNases.

Function and expression analysis of S-like RNases in citrus

It has been reported that the S-like RNases from plants are responsive to various stresses, such as virus infection, drought, and mechanical wounding (Perez-Amador et al. 2002; Salekdeh et al. 2002; Ohno and Ehara 2005). In this study, we found that the expression of *CsRNS1* was continuously up-regulated during fruit development and that at 240 DAF, its expression in a late-ripening orange mutant was remarkably higher than in wild type (Fig. 3). Furthermore, we found eight MeJA-responsive *cis*-elements in the promoter region of *CsRNS1* (Table 3). There are a large number of publications indicating that MeJA induces senescence (Woo et al. 2001; Schommer et al. 2008). Consistent with S-like RNases contributing to senescence, Chai et al. (2011b) reported that the expression of an S-like RNase gene (*CgSL2*) from 'Zigui shatian' pummelois up-regulated during the senescence of ovaries. There is a 95% sequence identity between *CsRNS1* and *CgSL2*. These data provide evidence that *CsRNS1* is an S-like RNase gene that probably contributes to senescence or fruit development. More evidence that S-like RNases contribute to the development of embryos comes from *RNase Dre1* and *Dre2* from Zebrafish. The expression of these two S-like RNase genes was gradually increased when embryos were induced (Hillwig et al. 2009). We found that the expression of *CsRNS6* was only detectable in embryogenic callus (Fig. 2). These data imply that *CsRNS6* may act as an S-like RNase gene and involve in embryo development (Hillwig et al. 2009; Ambrosio et al. 2014).

Involvement of *CgRNS3* in the self-incompatibility of 'Shatian' pummelo

S-RNases accumulate it the style and act as female determinants of self-incompatibility in Solanaceae, Rosaceae,

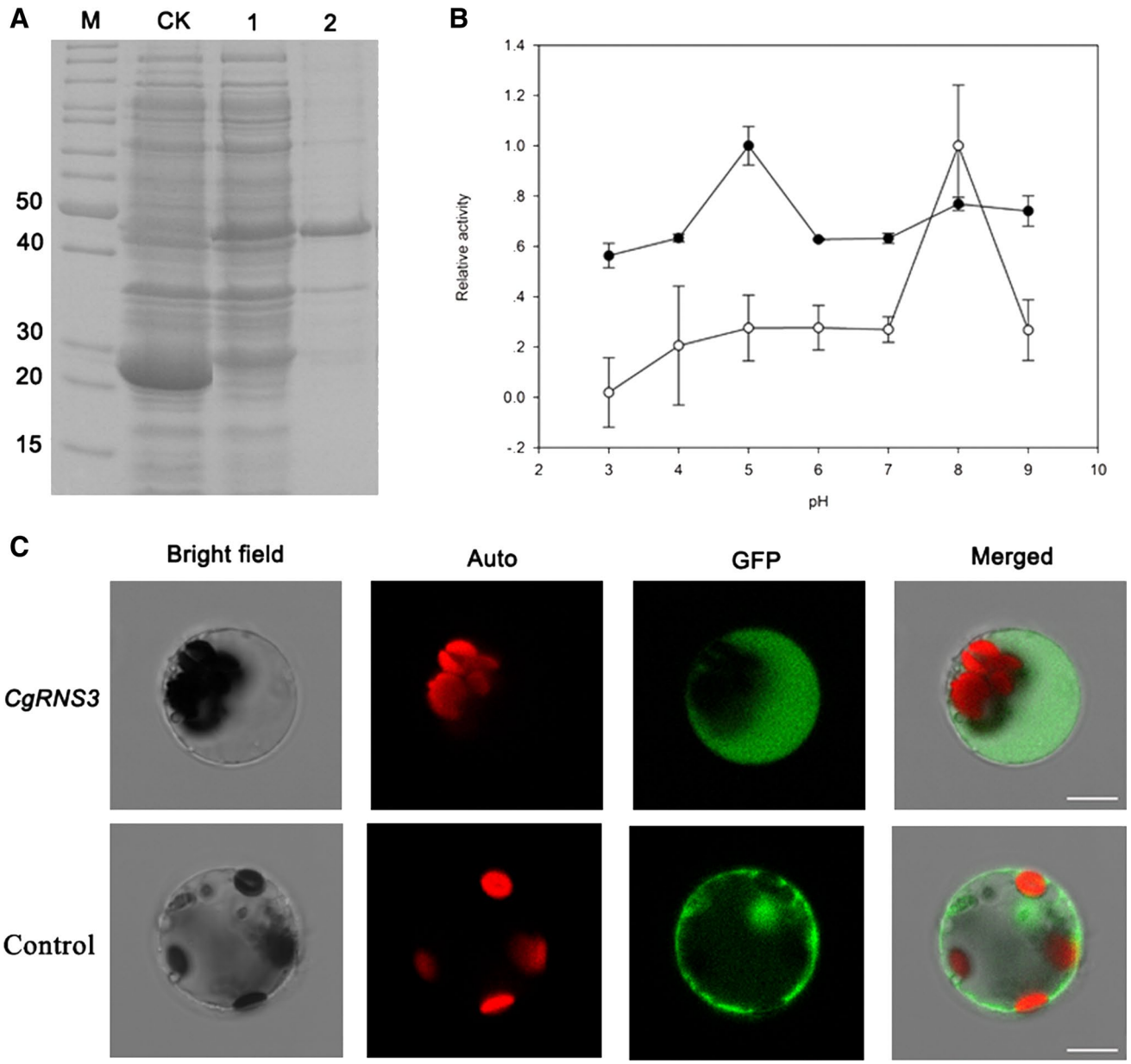

Fig. 7 RNase activity assay and the subcellular localization of CgRNS3. **a** Purification of the GST-CgRNS3 fusion protein. The crude lysate and the purified fusion protein were analyzed using SDS-PAGE. Lane 1, crude lysate; lane 2, purified recombinant protein. M, protein marker (labeled in kDa); CK, pGEX-6P-1 recombinant protein. **b** pH optimum of CgRNS3. The RNase assay was performed at several different pH values that ranged from 3 to 9. (*filled square*) recombinant protein. RNase A (*circle*). The mean values from three replicates are shown. *Error bars* indicate standard deviation (SD). **c** Subcellular localization of the full-length CgRNS3 fused to green fluorescent protein (GFP). *Bar* 10 μm

and Scrophulariaceae (Bredemeijer and Blaas 1981; Uchida et al. 2012). To screen for genes encoding S-RNases in citrus, we investigated the expression patterns of *CsRNS1* through *CsRNS9* by measuring the expression levels of these genes in the diverse tissues of the self-incompatible cultivar 'Shatian' pummelo. We observed style-specific expression only for *CsRNS3* (Fig. 4b). In addition, the molecular weight (25.7 kDa) and the highly basic pI (9.37) of *CsRNS3* are similar to the S-RNases that were identified in many other species (Anderson et al. 1986; Sassa et al. 1993; Asquini et al. 2011). Thus, we cloned the cDNA of *CgRNS3* from 'Shatian' pummelo and found only a few differences in the amino-acid sequences relative to *CsRNS3*. Results from quantitative RT-PCR and western blotting experiments indicate that *CgRNS3* is also expressed in the style (Fig. 6). Although the amino-acid sequences of S-RNases diverge

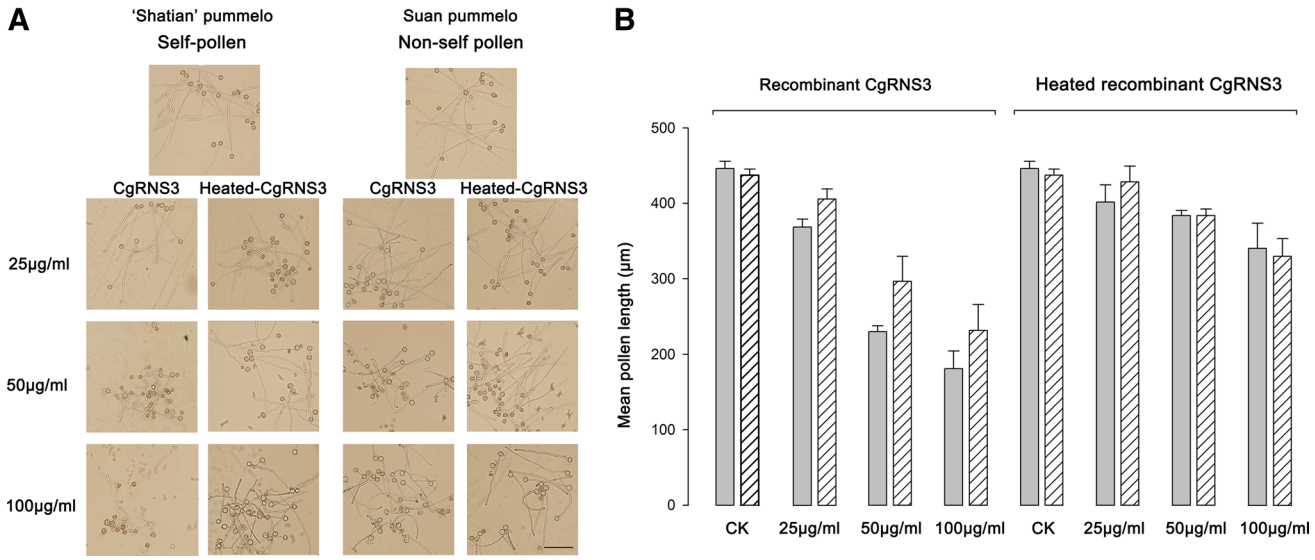

Fig. 8 Inhibitory effects of CgRNS3 on pollen tube growth *in vitro*. **a** Phenotypes of self ('Shatian' pummelo) and non-self (Suan pummelo) pollen tubes treated with CgRNS3. Control: untreated (CK) pollen. *Bar* 200 μm. **b** Effect of CgRNS3 and heated CgRNS3 on the growth of self (*gray bars*) and non-self (*stippled bars*) pollen tubes. The average values from three independent replicates are shown. *Error bars* indicate standard deviation (SD)

substantially, their protein topology is highly conserved. For instance, S-RNases from Solanaceae have five conserved regions (C1 to C5). These conserved regions, except for C4 conserved region, are also present in the S-RNases from Rosaceae. Interestingly, the C4 region of *CgRNS3* was distinguished from that of Rosaceae and Solanaceae. Two hypervariable regions are always observed in S-RNases from Solanaceae (HVa and HVb). In contrast, only one hypervariable region (RHV) is observed in S-RNases from Rosaceae (De Franceschi et al. 2012; Wu et al. 2013). The single hypervariable region of *CgRNS3* is distinct relative to the hypervariable regions of the S-RNases from Rosaceae. Indeed, the amino-acid sequence of *CgRNS3* is approximately 30% similar to all known S-RNases in NCBI database. Thus, we suspect that *CgRNS3* is a novel *S* allele relative to the *S* alleles from Rosaceae and Solanaceae.

The enzyme activity of CgRNS3 was also tested. Consistent with CgRNS3 serving as an S-RNase and in contrast to most RNase T2 enzymes, we found that the recombinant CgRNS3 that we purified from *E. coli* had a basic pH optimum (Irie 1999). The cytoplasmic localization is also consistent with CgRNS3 serving as an S-RNase (Li et al. 2016). Demonstrating S-RNase activity in an in vitro culture system is essential for establishing whether a candidate S-RNase contributes to self-incompatibility (Jahnen et al. 1989; Hiratsuka et al. 2001). Consistent with CgRNS3 serving as an S-RNase, the addition of the recombinant CgRNS3 protein to an in vitro culture system disturbed the growth of self-pollen tubes. Indeed, the CgRNS3-treated self-pollen tubes were abnormally shaped and were remarkably shortened in length relative to the untreated control. In contrast, the CgRNS3-treated non-self-pollen tubes grew normally without curved apex. Although the elongation of the non-self-pollen tubes was inhibited to some extent, the inhibition was less than the self-pollen tubes. We also tested whether CgRNS3 might also contribute to self-incompatibility in Suan pummelo by attempting to clone a cDNA encoding CgRNS3 from the styles of Suan pummelo. Indeed, the cDNA clone encoding CgRNS3 that we cloned from Suan pummelo is nearly identical to the cDNA clone encoding CgRNS3 that we cloned from 'Shatian' pummelo. Based on these data, we suggest that 'Shatian' and Suan pummelo have an *S* allele in common, which result in the inhibition of non-self-pollen tubes. We also found that the difference in the inhibition of growth caused by CgRNS3 in the self- and non-self-pollen tubes was reduced when the concentration of CgRNS3 was increased. Based on these data, we suggest that if the CgRNS3 protein was to accumulate to high levels in vivo, CgRNS3 would inhibit the growth of both self- and non-self-pollen tubes, which is consistent with the previous work (Meng et al. 2014). Furthermore, the heated protein without RNase activity alleviated the inhibition on the growth of pollen tubes. Although the previous studies have indicated that heating S-RNases from *N. alata* can dramatically increase its inhibitory activity and cause non-specific inhibition of pollen tube growth (Jahnen et al. 1989; Gray et al. 1991), we found that heat treating CgRNS3 dramatically reduced its ability to inhibit the growth of pollen tubes. Differences in the pollen of *C. grandis* and *N. alata* may explain these

results. Another possible explanation is different source of S-RNase protein. Instead of testing whether a purified recombinant protein could inhibit pollen tube growth, the previous studies tested whether a crude pistil extracts could inhibit pollen tube growth. A crude pistil extract might contain unknown factors that stimulate the growth of pollen tubes. The most parsimonious interpretation of our data is that after CgRNS3 enters pollen tubes, it accumulates in the cytoplasm and causes cytotoxic effects that depend on its RNase activity and that these cytotoxic effects disrupt the growth of self-pollen tubes in 'Shatian' pummelo.

In summary, we separately identified 9 and 7 RNase T2 homologs from sweet orange and clementine mandarin genomes. Based on phylogenetic comparisons and intron number comparisons, these putative RNase T2 enzymes were grouped into three clusters. This clustering allowed us to distinguish S-RNases from S-like RNases. We conclude that *CsRNS1* and *CsRNS6* are S-like RNases that are separately involved in senescence and embryo development. We conclude that *CgRNS3* is an S-RNase that is specifically expressed in the style and is required for self-incompatibility in 'Shatian' pummelo. We also conclude that *CgRNS3* is a novel S-RNase and that this new information will lead to deeper understanding of the mechanism of self-incompatibility in citrus.

Acknowledgements This research was financially supported by the National Natural Science Foundation of China (Nos. 31301760, 31521092, 31460507), the Special Fund for Agro-scientific Research in the Public Interest (201303093), and Scientific Research and Technology Development Program of Guangxi (Gui Ke He1599005-2-15). We also thank Prof. Zuoxiong Liu and Prof. Robert M. Larkin for help with English language editing.

Compliance with ethical standards

Conflict of interest The authors declare that none of the authors have a conflict of interest and that this article does not contain any studies with human participants or animals.

References

Ambrosio L, Morriss S, Riaz A, Bailey R, Ding J, MacIntosh GC (2014) Phylogenetic analyses and characterization of RNase X25 from *Drosophila melanogaster* suggest a conserved housekeeping role and additional functions for RNase T2 enzymes in protostomes. PLoS One 9:e105444

Anderson MA, Cornish EC, Mau SL, Williams EG, Hoggart R, Atkinson A, Bonig I, Grego B, Simpson R, Roche PJ, Haley JD, Penschow JD, Niall HD, Tregear GW, Coghlan JP, Crawford RJ, Clarke AE (1986) Cloning of cDNA for a stylar glycoprotein associated with expression of self incompatibility in *Nicotiana alata*. Nature 321:38–44

Asquini E, Gerdol M, Gasperini D, Igic B, Graziosi G, Pallavicini A (2011) S-RNase-like sequences in styles of *Coffea* (Rubiaceae). Evidence for S-RNase based gametophytic self-Incompatibility? Trop Plant Biol 4:237–249

Banović B, Šurbanovski N, Konstantinović M, Maksimović V (2009) Basic RNases of wild almond (*Prunus webbii*): cloning and characterization of six new *S*-RNase and one "non-*S* RNase" genes. J Plant Physiol 166:395–402

Bariola PA, Green PJ (1997) Plant ribonucleases. Ribonucleases: structures and functions. Academic Press, New York

Bredemeijer GMM, Blaas J (1981) S-specific proteins in styles of self-incompatible *Nicotiana alata*. Theor Appl Genet 59:185–190

Broothaerts W, Janssens GA, Proost P, Broekaert WF (1995) cDNA cloning and molecular analysis of two self-incompatibility alleles from apple. Plant Mol Biol 27:499–511

Cao H, Zhang J, Xu J, Ye J, Yun Z, Xu Q, Xu J, Deng X (2012) Comprehending crystalline β-carotene accumulation by comparing engineered cell models and the natural carotenoid-rich system of citrus. J Exp Bot 63:4403–4417

Caruso M, Merelo P, Distefano G, La Malfa S, Lo Piero AR, Tadeo FR, Talon M, Gentile A (2012) Comparative transcriptome analysis of stylar canal cells identifies novel candidate genes implicated in the self-incompatibility response of *Citrus clementina*. BMC Plant Biol 12:20

Chai L, Biswas MK, Ge X, Deng X (2010) Isolation, characterization, and expression analysis of an SKP1-like gene from 'Shatian' pummelo (*Citrus grandis* Osbeck). Plant Mol Biol Rep 28:569–577

Chai L, Ge X, Biswas MK, Deng X (2011a) Molecular analysis and expression of a floral organ-relative F-box gene isolated from 'Zigui shatian' pummelo (*Citrus grandis* Osbeck). Mol Biol Rep 38:4429–4436

Chai L, Ge X, Xu Q, Deng X (2011b) *CgSL2*, an S-like RNase gene in 'Zigui shatian' pummelo (*Citrus grandis* Osbeck), is involved in ovary senescence. Mol Biol Rep 38:1–8

Chalivendra SC, Lopez-Casado G, Kumar A, Kassenbrock AR, Royer S, Tovar-Mèndez A, Covey PA, Dempsey LA, Randle AM, Stack SM (2013) Developmental onset of reproductive barriers and associated proteome changes in stigma/styles of Solanum pennellii. J Exp Bot 64:265–279

Cui J, Wang H, Liu S, Zhu L, Qiu X, Jiang Z, Wang X, Liu Z (2014) SNP discovery from transcriptome of the Swimbladder of *Takifugu rubripes*. PLoS One 9:e92502

De Franceschi P, Dondini L, Sanzol J (2012) Molecular bases and evolutionary dynamics of self-incompatibility in the Pyrinae (Rosaceae). J Exp Bot 63:4015–4032

De Nettancourt D (2001) Incompatibility and incongruity in wild and cultivated plants. Springer-Verlag, Berlin

Deng X (1987) Studies on the isolation, regeneration and fusion of protoplast in *Citrus*. Dissertation, Huazhong Agriculture University

Deshpande RA, Shankar V (2002) Ribonucleases from T2 family. Crit Rev Microbiol 28:79–122

Gasteiger E, Hoogland C, Gattiker A, Wilkins MR, Appel RD, Bairoch A (2005) Protein identification and analysis tools on the ExPASy server. In Walker JM (ed) The Proteomics Protocols Handbook. Humana Press, pp 571–607

Gray JE, Mcclure BA, Bönig I, Anderson MA, Clarke AE (1991) Action of the style product of the self-incompatibility gene of *Nicotiana alata* (S-RNase) on in vitro-grown pollen tubes. Plant Cell 3:271–283

Guo A, Zhu Q, Chen X, Luo J (2007) GSDS: a gene structure display server. Yi Chuan 29:1023–1026

Hillwig MS, Rizhsky L, Wang Y, Umanskaya A, Essner JJ, MacIntosh GC (2009) Zebrafish RNase T2 genes and the evolution of secretory ribonucleases in animals. BMC Evol Biol 9:170

Hiratsuka S, Zhang SL, Nakagawa E, Kawai Y (2001) Selective inhibition of the growth of incompatible pollen tube by S-protein in the Japanese pear. Sex Plant Reprod 13:209–215

Hua ZH, Fields A, Kao Th (2008) Biochemical models for S-RNase-based self-incompatibility. Mol Plant 1:575–585

Huang S, Lee HS, Karunanandaa B, Kao TH (1994) Ribonuclease activity of *Petunia inflata* S proteins is essential for rejection of self-pollen. Plant Cell 6:1021–1028

Igic B, Kohn JR (2001) Evolutionary relationships among self-incompatibility RNases. Proc Natl Acad Sci USA 98:13167–13171

Irie M (1999) Structure-function relationships of acid ribonucleases: lysosomal, vacuolar, and periplasmic enzymes. Pharmacol Ther 81:77–89

Isaacson T, Damasceno CM, Saravanan RS, He Y, Catalá C, Saladié M, Rose JK (2006) Sample extraction techniques for enhanced proteomic analysis of plant tissues. Nat Protoc 1:769–774

Jahnen W, Lush WM, Clarke AE (1989) Inhibition of in vitro pollen tube growth by isolated S-glycoproteins of *Nicotiana alata*. Plant Cell 1:501–510

Kawata Y, Sakiyama F, Hayashi F, Kyogoku Y (1990) Identification of two essential histidine residues of ribonuclease T2 from *Aspergillus oryzae*. Eur J Biochem 187:255–262

Lee HS, Singh A, Kao T (1992) RNase X2, a pistil-specific ribonuclease from *Petunia inflata*, shares sequence similarity with solanaceous S proteins. Plant Mol Biol 20:1131–1141

Lee HS, Huang S, Kao TH (1994) S proteins control rejection of incompatible pollen in *petunia inflata*. Nature 367:560–563

Lescot M, Déhais P, Thijs G, Marchal K, Moreau Y, Van de Peer Y, Rouzé P, Rombauts S (2002) PlantCARE, a database of plant cis-acting regulatory elements and a portal to tools for in silico analysis of promoter sequences. Nucleic Acids Res 30:325–327

Li P, Miao HX, Ma YW, Wang L, Hu GB, Ye ZX, Zhao JT, Qin YH (2015) *CrWSKP1*, an SKP1-like Gene, is involved in the self-Incompatibility reaction of "Wuzishatangju" (*Citrus reticulata* Blanco). Int J Mol Sci 16:21695–21710

Li J, Zhang Y, Song Y, Zhang H, Fan J, Li Q, Zhang D, Xue Y (2016) Electrostatic potentials of the S-locus F-box proteins contribute to the pollen S specificity in self-incompatibility in *Petunia hybrida*. Plant J. doi:10.1111/tpj.13318

Liang LZ, Lai Z, Ma WS, Zhang YS, Xue YB (2002) *AhSL28*, a senescence-and phosphate starvation-induced S-like RNase gene in Antirrhinum. Biochim Biophys Acta 1579:64–71

Liang M, Yang X, Li H, Su S, Yi H, Chai L, Deng X (2015) De novo transcriptome assembly of pummelo and molecular marker development. PLoS ONE 10:e0120615

Lin Z, Eaves DJ, Sanchez Moran E, Franklin FCH, Franklin Tong VE (2015) The *Papaver rhoeas* S determinants confer self-incompatibility to *Arabidopsis thaliana* in planta. Science 350:684–687

Liu J, Deng X (2002) Regeneration and analysis of citrus interspecific mixoploid hybrid plants from asymmetric somatic hybridization. Euphytica 125:13–20

Liu Y, Liu Q (2006) Efficient isolation of RNA from fruit peel and pulp of ripening navel orange (*Citrus sinensis* Osbeck). Dissertation, Journal of Huazhong Agricultural University

Luhtala N, Parker R (2010) T2 Family ribonucleases: ancient enzymes with diverse roles. Trends Biochem Sci 35:253–259

Masashi Y, Tatsuya K, Shigeto T (2006) Self-and cross-incompatibility of various citrus accessions. J Jpn Soc Hortic Sci 75:372–378

McClure BA, Haring V, Ebert PR, Anderson MA, Simpson RJ, Sakiyama F, Clarke AE (1989) Style self-incompatibility gene products of *Nicotlana alata* are ribonucleases. Nature 342:955–957

McCubbin AG, Kao Th (2000) Molecular recognition and response in pollen and pistil interactions. Annu Rev Cell Dev Biol 16:333–364

Meng D, Gu Z, Yuan H, Wang A, Li W, Yang Q, Zhu Y, Li T (2014) The microtubule cytoskeleton and pollen tube Golgi vesicle system are required for in vitro S-RNase internalization and gametic self-incompatibility in apple. Plant Cell Physiol 55:977–989

Miao HX, Qin YH, da Silva JAT, Ye ZX, Hu GB (2011) Cloning and expression analysis of S-RNase homologous gene in Citrus reticulata Blanco cv. Wuzishatangju. Plant Sci 180:358–367

Miao HX, Ye ZX, Qin YH, Hu GB (2013) Molecular characterization and expression analysis of S1 self-incompatibility locus-linked pollen 3.15 gene in *Citrus reticulata*. J Integr Plant Biol 55:443–452

Miao HX, Ye ZX, Hu GB, Qin YH (2015) Comparative transcript profiling of gene expression between self-incompatible and self-compatible mandarins by suppression subtractive hybridization and cDNA microarray. Mol Breed 35:1–15

Murfett J, Atherton TL, Mou B, Gassert CS, Mcclure BA (1994) S-RNase expressed in transgenic *Nicotiana* causes S-allele-specific pollen rejection. Nature 367:563–566

Ngo B (2001) Study on the self-incompatibility in Citrus (Rutaceae) with special emphases on the pollen tube growth and allelic variation. Dissertation, Kyushu University

Nishimura E, Jumyo S, Arai N, Kanna K, Kume M, J-i Nishikawa, J-i Tanase, Ohyama T (2014) Structural and functional characteristics of S-like ribonucleases from carnivorous plants. Planta 240:147–159

Ohno H, Ehara Y (2005) Expression of ribonuclease gene in mechanically injured or virus-inoculated *Nicotiana tabacum* leaves. Tohoku J Agric Res 55:99–109

Pan Z, Liu Q, Yun Z, Guan R, Zeng W, Xu Q, Deng X (2009) Comparative proteomics of a lycopene-accumulating mutant reveals the important role of oxidative stress on carotenogenesis in sweet orange (*Citrus sinensis* [L.] osbeck). Proteomics 9:5455–5470

Perez-Amador MA, Leon J, Green PJ, Carbonell J (2002) Induction of the arginine decarboxylase ADC2 gene provides evidence for the involvement of polyamines in the wound response in *Arabidopsis*. Plant Physiol 130:1454–1463

Roalson EH, McCubbin AG (2003) S-RNases and sexual incompatibility: structure, functions, and evolutionary perspectives. Mol Phylogenet Evol 29:490–506

Salekdeh GH, Siopongco J, Wade L, Ghareyazie B, Bennett J (2002) A proteomic approach to analyzing drought-and salt-responsiveness in rice. Field Crops Research 76:199–219

Sassa H, Hirano H, Ikehashi H (1992) Self-incompatibility-related RNases in styles of Japanese pear (*Pyrus serotina* Rehd.). Plant Cell Physiol 33:811–814

Sassa H, Hirano H, Ikehashi H (1993) Identification and characterization of stylar glycoproteins associated with self-incompatibility genes of Japanese pear, *Pyrus serotina* Rehd. Mol Gen Genet 241:17–25

Schommer C, Palatnik JF, Aggarwal P, Chételat A, Cubas P, Farmer EE, Nath U, Weigel D (2008) Control of jasmonate biosynthesis and senescence by miR319 targets. PLoS Biol 6:e230

Takayama S, Isogai A (2005) Self-incompatibility in plants. Ann Rev Plant Biol 56:467–489

Tamura K, Peterson D, Peterson N, Stecher G, Nei M, Kumar S (2011) MEGA5: molecular evolutionary genetics analysis using maximum likelihood, evolutionary distance, and maximum parsimony methods. Mol Biol Evol 28:2731–2739

Tao R, Yamane H, Sassa H, Mori H, Gradziel TM, Dandekar AM, Sugiura A (1997) Identification of stylar RNases associated with gametophytic self-incompatibility in Almond (*Prunus dulcis*). Plant Cell Physiol 38:304–311

Tao R, Yamane H, Sugiura A, Murayama H, Sassa H, Mori H (1999) Molecular typing of S-alleles through identification, characterization and cDNA cloning for S-RNases in sweet cherry. J Am Soc Hortic Sci 124:224–233

Taylor CB, Bariola PA, Raines RT, Green PJ (1993) *RNS2*: a senescence-associated RNase of *Arabidopsis* that diverged from the S-RNases before speciation. Proc Natl Acad Sci USA 90:5118–5122

Uchida A, Takenaka S, Sakakibara Y, Kurogi S, Honsho C, Sassa H, Suiko M, Kunitake H (2012) Comprehensive analysis of expressed proteins in the different stages of the style development of self-incompatible 'Hyuganatsu' (*Citrus tamurana* hort. ex Tanaka). J Jpn Soc Hortic Sci 81:150–158

Velasco R, Licciardello C (2014) A genealogy of the citrus family. Nat Biotechnol 32:640–642

Wang CL, Xu GH, Jiang XT, Chen G, Wu J, Wu HQ, Zhang SL (2009) S-RNase triggers mitochondrial alteration and DNA degradation in the incompatible pollen tube of *Pyrus pyrifolia* in vitro. Plant J 57:220–229

Waugh DS (2005) Making the most of affinity tags. Trends Biotechnol 23:316–320

Wei JY, Li AM, Li Y, Wang J, Liu XB, Liu LS, Xu ZF (2006) Cloning and characterization of an RNase-related protein gene preferentially expressed in rice stems. Biosci Biotechnol Biochem 70:1041–1045

Woo HR, Chung KM, Park JH, Oh SA, Ahn T, Hong SH, Jang SK, Nam HG (2001) *ORE9*, an F-box protein that regulates leaf senescence in *Arabidopsis*. Plant Cell 13:1779–1790

Wu J, Gu C, Khan MA, Wu J, Gao Y, Wang C, Korban SS, Zhang S (2013) Molecular determinants and mechanisms of gametophytic self-Incompatibility in fruit trees of Rosaceae. Crit Rev Plant Sci 32:53–68

Wu GA, Prochnik S, Jenkins J, Salse J, Hellsten U, Murat F, Perrier X, Ruiz M, Scalabrin S, Terol J (2014a) Sequencing of diverse mandarin, pummelo and orange genomes reveals complex history of admixture during citrus domestication. Nat Biotechnol 32:656

Wu J, Xu Z, Zhang Y, Chai L, Yi H, Deng X (2014b) An integrative analysis of the transcriptome and proteome of the pulp of a spontaneous late-ripening sweet orange mutant and its wild type improves our understanding of fruit ripening in citrus. J Exp Bot 65:1651–1671

Xu Q, Chen LL, Ruan X, Chen D, Zhu A, Chen C, Bertrand D, Jiao W-B, Hao B-H, Lyon MP (2013) The draft genome of sweet orange (*Citrus sinensis*). Nat Genet 45:59–66

Yoo SD, Cho YH, Sheen J (2007) *Arabidopsis* mesophyll protoplasts: a versatile cell system for transient gene expression analysis. Nat Protoc 2:1565–1572

Zhang SW, Ding F, He XH, Luo C, Huang GX, Hu Y (2015) Characterization of the 'Xiangshui' lemon transcriptome by de novo assembly to discover genes associated with self-incompatibility. Mol Genet Genomics 290:365–375